

Mutant p53 cooperates with ETS2 to promote etoposide resistance

Phi M. Do,¹ Lakshman Varanasi,¹ Songqing Fan,² Chunyang Li,² Iwona Kubacka,³ Virginia Newman,¹ Krishna Chauhan,¹ Silvano Rakeem Daniels,¹ Maurizio Bocchetta,⁴ Michael R. Garrett,¹ Runzhao Li,^{2,5} and Luis A. Martinez^{1,5}

¹Department of Biochemistry, University of Mississippi Cancer Institute, University of Mississippi Medical Center, Jackson, Mississippi 39216, USA; ²Department of Hematology and Medical Oncology, Winship Cancer Institute, Emory University School of Medicine, Atlanta, Georgia 30322, USA; ³University of Texas Medical Branch, Galveston, Texas 77554, USA; ⁴Oncology Institute, Institute of Signal Transduction, Loyola University Chicago, Maywood, Illinois 60153, USA

Mutant p53 (mtp53) promotes chemotherapy resistance through multiple mechanisms, including disabling proapoptotic proteins and regulating gene expression. Comparison of genome wide analysis of mtp53 binding revealed that the ETS-binding site motif (EBS) is prevalent within predicted mtp53-binding sites. We demonstrate that mtp53 regulates gene expression through EBS in promoters and that ETS2 mediates the interaction with this motif. Importantly, we identified TDP2, a 5'-tyrosyl DNA phosphodiesterase involved in the repair of DNA damage caused by etoposide, as a transcriptional target of mtp53. We demonstrate that suppression of TDP2 sensitizes mtp53-expressing cells to etoposide and that mtp53 and TDP2 are frequently overexpressed in human lung cancer; thus, our analysis identifies a potentially "druggable" component of mtp53's gain-of-function activity.

[Keywords: TDP2; cancer; p53]

Supplemental material is available for this article.

Received October 20, 2011; revised version accepted March 9, 2012.

One of the definitive characteristics of the mutant p53 (mtp53) protein is that it can alter the cellular phenotype, resulting in the acquisition of gain-of-function activities such as abnormal cell growth, suppression of apoptosis, chemotherapy resistance, increased angiogenesis, and metastasis (Lozano and Zambetti 2005; Li and Prives 2007; Brosh and Rotter 2009; Muller et al. 2011). Protein-protein interactions appear to underlie several of the gain-of-function activities of mtp53 (Li and Prives 2007; Brosh and Rotter 2009). For example, mtp53 can interact with its family members, p63 and p73, and disable their ability to induce apoptosis (Di Como et al. 1999; Marin et al. 2000; Strano et al. 2000, 2002; Gaiddon et al. 2001; Bergamaschi et al. 2003; Irwin et al. 2003; Lang et al. 2004). mtp53 can also interact with other transcription factors (such as NF-Y, E2F1, VDR, and p63) and thereby can be recruited to target genes that have consensus binding sites for these transcription factors (Di Agostino et al. 2006; Adorno et al. 2009; Fontemaggi et al. 2009; Stambolsky et al. 2010). Notably, some of these interactions help explain how the mtp53 protein can deregulate gene expression

and promote abnormal cell growth, angiogenesis, and metastasis (Di Agostino et al. 2006; Adorno et al. 2009; Fontemaggi et al. 2009; Muller et al. 2009, 2011). However, thus far, none of these transcription factors have been shown to play a fundamental role in regulating the expression of genes that can confer chemotherapy resistance by modulating the response to DNA damage. The main goal of this study was to identify a transcriptional regulatory mechanism through which mtp53 can promote chemotherapy resistance.

Results

Identification of mtp53 target genes

To identify transcriptional targets of mtp53, we employed two different approaches: chromatin immunoprecipitation (ChIP)-on-chip and ChIP combined with deep sequencing (ChIP-seq). The ChIP-on-chip was performed with Nimblegen arrays that have oligonucleotide probes for all of the promoters in the human genome (Nimblegen Promoter Arrays). The ChIP-seq analysis was performed using the Illumina platform. We conducted these analyses in the Li-Fraumeni cell line MDAH087, which expresses only the R248W mtp53 protein (Bischoff et al. 1990). The ChIP-on-chip analysis identified 1711 mtp53-

⁵Corresponding authors.
E-mail lmartinez@umc.edu.
E-mail r.li@emory.edu.

Article is online at <http://www.genesdev.org/cgi/doi/10.1101/gad.181685.111>.

binding sites that did not show significant enrichment in the promoter array hybridized with DNA that coimmunoprecipitated with a control (Ct) antibody and had a false discovery rate (FDR) of $\leq 0.8\%$. The ChIP-seq approach identified 6062 binding sites ($\text{FDR} \leq 5\%$), with 4393 being present in the promoter region of genes. Thus, both analyses indicate that mtp53 binds a high number of promoter regions (Fig. 1A). Notably, ChIP-seq, which is a global and unbiased method of identifying binding sites in the genome, indicated that the vast majority of the binding sites for mtp53 are in promoter regions, suggesting a nonrandom pattern for association with DNA.

We were specifically interested in mtp53 DNA-binding sites located in promoter regions and thus focused our analysis on the overlapping genes from these data sets. Comparison of the ChIP-on-chip and ChIP-seq data sets indicated that there were 602 overlapping promoters. The differences in the data sets may be due to the use of distinct algorithms for data processing and to differences in the sensitivity and specificity of each platform (Fig. 1A). However, the fact that these 602 promoter regions in the composite data set were identified with two different experimental approaches indicates that they are high-confidence binding sites for mtp53.

We randomly selected a set of genes to validate the composite data set (Supplemental Fig. S1). PCR analysis

of ChIP DNA confirmed that mtp53 associates with almost all of these promoter regions (Fig. 1B; Supplemental Fig. S2A,B; Supplemental Table S2). Analysis of mtp53 association with distal promoter regions revealed a lack of binding, indicating that mtp53 specifically associates with the predicted binding sites (Supplemental Fig. S2A). Next, we tested whether siRNA knockdown of mtp53 altered their expression. To reduce the bias of tissue-specific transcriptional regulation by mtp53, we did this analysis in two different cell lines: the MDAH087 cells in which the initial ChIP work was performed and the MIA PaCa-2 pancreatic cell line, which expresses the same R248W mtp53. Quantitative PCR (qPCR) analysis revealed that mtp53 knockdown caused changes in the expression in most of these target genes (Fig. 1C,D). In general, mtp53 knockdown in both cell lines produced similar changes in target gene expression, although the magnitude varied. We noted that the magnitude in change for some of the genes was modest, which could be due to the fact that the mtp53 knockdown did not completely eliminate the protein (Supplemental Fig. S2C). Nevertheless, the fact that mtp53 binds to the promoters of these genes and that mtp53 knockdown alters their expression suggests that they are direct transcriptional targets.

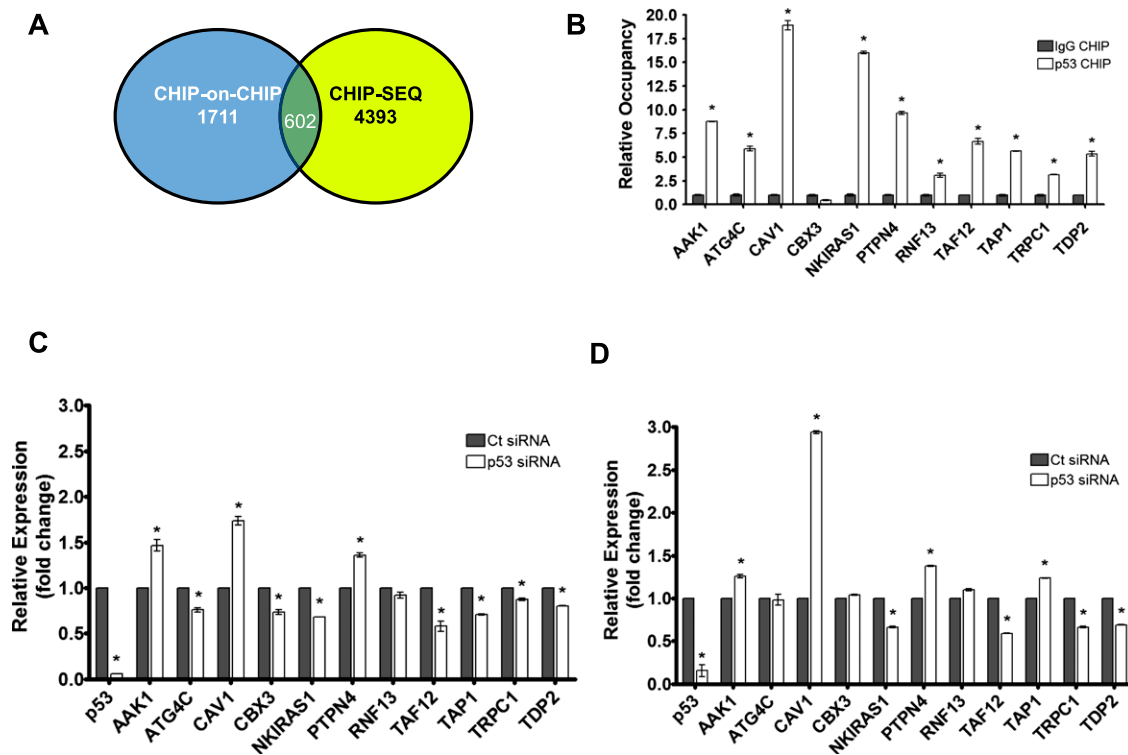


Figure 1. ChIP-on-chip and ChIP-seq analysis of mtp53 binding. (A) ChIP-on-chip and ChIP-seq analysis performed for mtp53 using MDAH087 cells revealed sites that were unique and common to both platforms. Analysis of ChIP-on-chip and ChIP-seq data revealed 1711 and 4393 mtp53-occupied promoters, with an overlap of 602 promoters. (B) Validation of 11 promoter regions predicted by ChIP-on-chip and ChIP-seq by qPCR showing relative occupancy compared with control IgG (mean \pm SEM; [*] P -value ≤ 0.01 vs. IgG ChIP). The gene name listed represents the ORF nearest to the predicted mtp53-binding site. Change in expression of select genes after p53 knockdown in MDAH087 (C) and MIA PaCa-2 (D). Expression analysis by qPCR of the same 11 putative mtp53 target genes (and p53) was performed on cells transfected with either control (Ct) or p53 siRNA (mean \pm SEM; [*] P -value ≤ 0.05 vs. control siRNA).

DNA-binding partner for mtp53

Mutations in the DNA-binding domain of p53 cause it to lose the ability to bind the wild-type p53 consensus sequence (Kern et al. 1991). Indeed, the analysis of the R248W mtp53-bound sequences, using the p53MH algorithm, failed to detect a wild-type p53 consensus binding site (almost all scores obtained were ≤ 70) (Hoh et al. 2002). Moreover, comparison of our set of 602 promoters with genome-wide analyses of wild-type p53 binding (Wei et al. 2006; Smeenk et al. 2008; Botcheva et al. 2011) indicated that $<5.1\%$ were within 5 kb and 1.7% were within 150 bases of our predicted mtp53-binding sites (Table 1; Supplemental Table S3). Thus, mtp53's association with these genomic loci does not appear to depend on vestigial wild-type p53 DNA-binding activity. (Table 1; Supplemental Table S3). Although the mtp53 protein appears to lack sequence-specific DNA-binding activity, it can still be recruited to promoters through protein–protein interactions with other transcription factors. Therefore, we speculated that protein–protein interactions may underlie its association with these promoter regions, and so if this was the case, then it would be expected that a consensus sequence for this putative mtp53-binding partner is overrepresented in the composite target gene data set. We analyzed the ChIP-on-chip and ChIP-seq predicted binding sites from the overlapping promoters data set using the Multiple Em for Motif Elicitation (MEME) suite (Bailey and Elkan 1994; Sun et al. 2010). There were multiple motifs that were found to be overrepresented in the predicted binding sites, but the most predominant was GGAAR, which is similar to an ETS-binding site (EBS) (Fig. 2A; Supplemental Fig. S3). Specifically, we found that the GGAAR sequence occurred in 74.2% (1269 of 1711) of ChIP-on-chip, 44.9% (1973 of 4393) of ChIP-seq, and 50% (301 of 602) of the composite (overlapping) data sets (Fig. 2B). Additionally, the TOMTOM motif comparison tool of the MEME suite predicted the binding of three

members of the ETS family—ETS1, ETS2, and SPI-1/PU.1—due to the high similarity of their consensus binding sites to the motif that we discovered (Fig. 2A).

We focused our analysis on the 602 promoters that overlapped between our two platforms. Of these promoters, we determined that 301 have predicted EBS motifs within the mtp53-binding site (Fig. 2B; Supplemental Table S3). In order to confirm that the EBS motifs present in these 301 mtp53-binding sites were indeed occupied by ETS proteins, we compared our data set with data sets from previously reported genome-wide analyses of ETS1 binding (Hollenhorst et al. 2009). We observed that in this subset of mtp53-binding sites, 264 (43.8%) are reported to be occupied by ETS proteins within 150 base pairs (bp) (Fig. 2C; Table 1; Supplemental Table S3). In contrast, an analysis of previously published wild-type p53-binding sites from three different cell lines did not reveal a similar overrepresentation of the EBS. Specifically, we observed that within a 150-bp region surrounding the wild-type p53-binding sites, an EBS was present in 18.2% in IMR-90, 2.0% in HCT116, and 0.5% in U2OS (Table 1; Supplemental Table S4). It is also interesting to note that of the wild-type p53 promoters that have an EBS, only seven (0.02%), two (0.01%), and seven (0.02%) promoters in IMR90, HCT116, and U2OS cells, respectively, are present in our data set of mtp53-binding sites (Supplemental Table S3). Therefore, these mtp53-binding sites represent novel target genes of the mutant protein. Given the prevalence of the EBS in the mtp53-binding sites, we decided to study the interaction of the ETS proteins with mtp53.

The ETS gene family is composed of 28 members, and their defining feature is the presence of the ETS domain, which is involved in DNA binding (Mavrothalassitis and Ghysdael 2000; Hollenhorst et al. 2011). Given the high degree of homology of their ETS domains, all of the ETS family members bind to a 4-nucleotide (nt) core sequence (GGAA), although other sequences adjacent to this motif and protein–protein interactions dictate the specificity toward their target genes (Hollenhorst et al. 2009). Pre-

Table 1. Comparison of predicted mtp53-binding site with other genome-wide ChIP analysis

	Wild-type p53 ^a (<i>n</i> = 411)	Wild-type p53 ^b (<i>n</i> = 202)	Wild-type p53 ^c (<i>n</i> = 428)	ETS1 ^d (<i>n</i> = 14825)
Mtp53 (≤ 5000 bp; <i>n</i> = 602)	21 (5.1%) ^e	6 (3.0%) ^e	10 (2.3%) ^e	325 (54.0%) ^f
Mtp53 (≤ 1000 bp; <i>n</i> = 602)	17 (4.1%) ^e	3 (1.5%) ^e	1 (0.2%) ^e	303 (50.3%) ^f
Mtp53 (≤ 150 bp; <i>n</i> = 602)	7 (1.7%) ^e	2 (1.0%) ^e	0 (0.0%) ^e	264 (43.9%) ^f
ETS1 ^d (≤ 5000 bp; <i>n</i> = 14,825)	204 (49.6%) ^e	35 (17.3%) ^e	61 (14.3%) ^e	—
ETS1 ^d (≤ 1000 bp; <i>n</i> = 14,825)	166 (40.4%) ^e	12 (5.9%) ^e	27 (6.3%) ^e	—
ETS1 ^d (≤ 150 bp; <i>n</i> = 14,825)	75 (18.2%) ^e	4 (2.0%) ^e	2 (0.5%) ^e	—

ChIP-on-chip and ChIP-seq overlap binding sites were compared with published wild-type p53- and ETS1-binding sites. (*n*) Number of binding sites within the promoter regions (-4 kb to $+1$ kb relative to the TSS). The data represent the number of promoter-binding sites of the sources (wild-type p53 or ETS1) compared with mtp53- or ETS1-binding sites within the indicated base pair (bp) distance.

^aNormal fibroblast cell line IMR90; wild-type p53-binding sites were identified by ChIP-seq (Botcheva et al. 2011).

^bColorectal cancer cell line HCT116; wild-type p53-binding sites were identified using ChIP-PET sequencing (Wei et al. 2006).

^cOsteosarcoma cell line U2OS; wild-type p53-binding sites were identified using ChIP-on-chip (Smeenk et al. 2008).

^dJurkat T-cell line; ETS1-binding sites were identified by ChIP-seq (Hollenhorst et al. 2009).

^ePercentage of predicted wild-type p53-binding sites that overlap mtp53- or ETS1-binding sites within the indicated base pair (bp) distance.

^fPercentage of predicted mtp53-binding sites that overlap ETS1-binding sites within the indicated base pair (bp) distance.

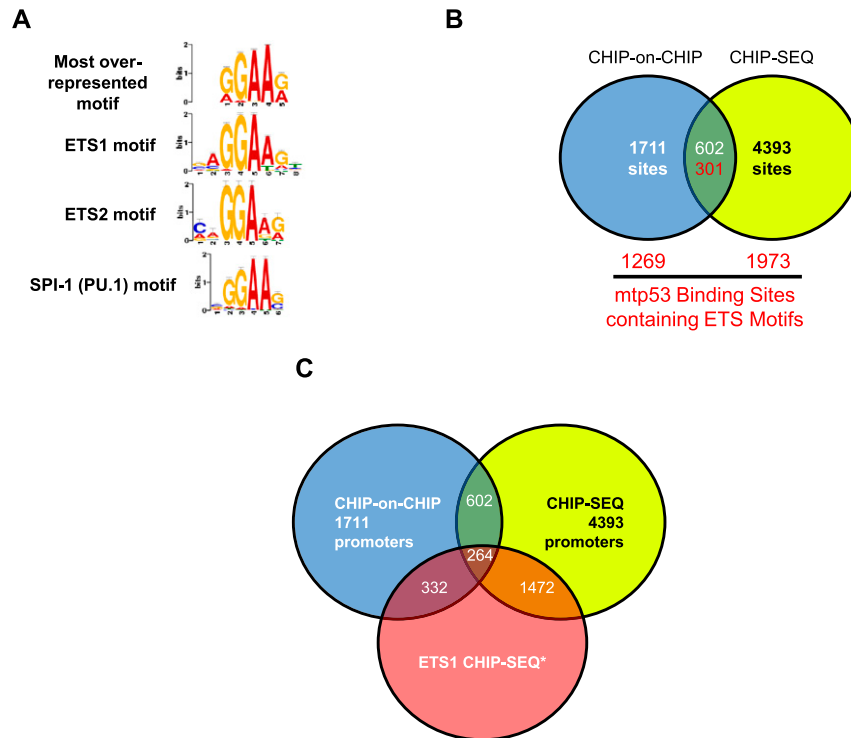


Figure 2. Motif alignment and binding prediction. (A) The EBS is the most over-represented motif discovered in the MEME alignment. The 602 predicted mtp53-binding sites from the ChIP-seq data set alone were aligned using the MEME suite. The most overrepresented motif (GGAAR) was found to be highly specific for the ETS family of proteins' binding sites. (B) Analysis of the prevalence of EBSs in predicted mtp53-binding sites across different platforms. Further analysis of the ChIP-on-chip and ChIP-seq data sets revealed high prevalence of the MEME-discovered ETS motif within predicted mtp53-binding sites in both platforms; the motif accounts for 74.2% of ChIP-on-chip (1269 out of 1711), 44.9% of ChIP-seq (1973 out of 4393), and 50.0% of the overlapping promoters (301 out of 602). (C) Data mining of published ETS1 ChIP-seq data revealed a similar overlap of ETS1- and predicted mtp53-binding sites. By comparing our ChIP-on-chip and ChIP-seq data sets with ETS1 ChIP-seq data as reported by Hollenhorst et al. (2009), we demonstrated that a majority of our predicted mtp53 binding overlap ETS1 binding within ≤ 150 bp.

vious studies have suggested that ETS1 can regulate the activity of both wild-type p53 and mtp53, although there are discrepancies in regard to whether this requires a direct interaction between the proteins (Pastorcic and Das 2000; Sampath et al. 2001; Xu et al. 2002; Kim et al. 2003; Gu et al. 2004; Sankala et al. 2011). Since the EBS sequence identified in our analysis may be bound by other ETS family members, we considered the possibility that other ETS family members might be involved (Hollenhorst et al. 2009). Therefore, we investigated the involvement of the three ETS family members implicated by the TOM-TOM motif analysis. The ETS1 and ETS2 proteins are very similar to each other, with an overall 55% identity and a 96% identity in their DNA-binding domain (Charlot et al. 2010; Hollenhorst et al. 2011). In contrast, SPI-1/PU.1 is more divergent and exhibits a 30% identity only in the ETS DNA-binding domain (Charlot et al. 2010; Hollenhorst et al. 2011). As a first step, we assessed whether these proteins associated with mtp53 in an endogenous setting in two different cell lines: the MDAH087 (Li-Fraumeni fibroblasts) and MIA PaCa-2 (pancreatic cancer). We immunoprecipitated mtp53 and detected the coimmunoprecipitating proteins by Western blot. Our analysis revealed that both ETS1 and ETS2 coimmunoprecipitate with mtp53 (Fig. 3A,B). We also examined the association of vitamin D receptors (VDR), a protein previously shown to bind mtp53 (Stambolsky et al. 2010). We observed a very weak but reproducible interaction between mtp53 and VDR (Fig. 3A,B). In contrast, the interaction between the ETS proteins, especially ETS2, and mtp53 was more robust (Fig. 3A,B). The ETS2 protein is highly unstable (20-min half-life), and we had

difficulty detecting it in whole-cell lysates using different antibodies (Fujiwara et al. 1988). However, we noticed that in both cell lines, there was a marked difference in ETS2 levels detected in the p53 immunoprecipitation relative to the levels detected in the whole-cell lysate (Fig. 3A,B). One explanation for these data is that ETS2 may have a higher affinity for mtp53. To validate these results, we also performed immunoprecipitations with antibodies against ETS1, ETS2, ETS1/ETS2 (i.e., recognizes an epitope common to both), PU.1, and VDR. In line with our observations above, ETS2 coimmunoprecipitated more mtp53 than the other transcription factors (Supplemental Fig. S4A,B). The PU.1 antibody brought down a minor amount of mtp53 protein that was slightly above background (Supplemental Fig. S4A,B). We noted that we could detect ETS1 in the ETS2 immunoprecipitation and vice versa. Previous reports have indicated that ETS1 and ETS2 interact with each other, thus it is not unexpected that they appear to coimmunoprecipitate (Basuyaux et al. 1997; Babayeva et al. 2010). We can conclude from these results that mtp53 can form complexes with either ETS1 or ETS2, although it appears to preferentially associate with ETS2. We also assessed whether endogenous wild-type p53 from U2OS cells could interact with ETS1 and ETS2 (Fig. 3C; Supplemental Fig. S4C). Although we were unable to detect an interaction between wild-type p53 and ETS1, we did detect ETS2 in the p53 immunoprecipitation and vice versa (Fig. 3C; Supplemental Fig. S4C).

In order to determine whether mtp53 was directly associating with these proteins, we incubated *in vitro* transcribed/translated recombinant wild-type p53 and mtp53

Do et al.

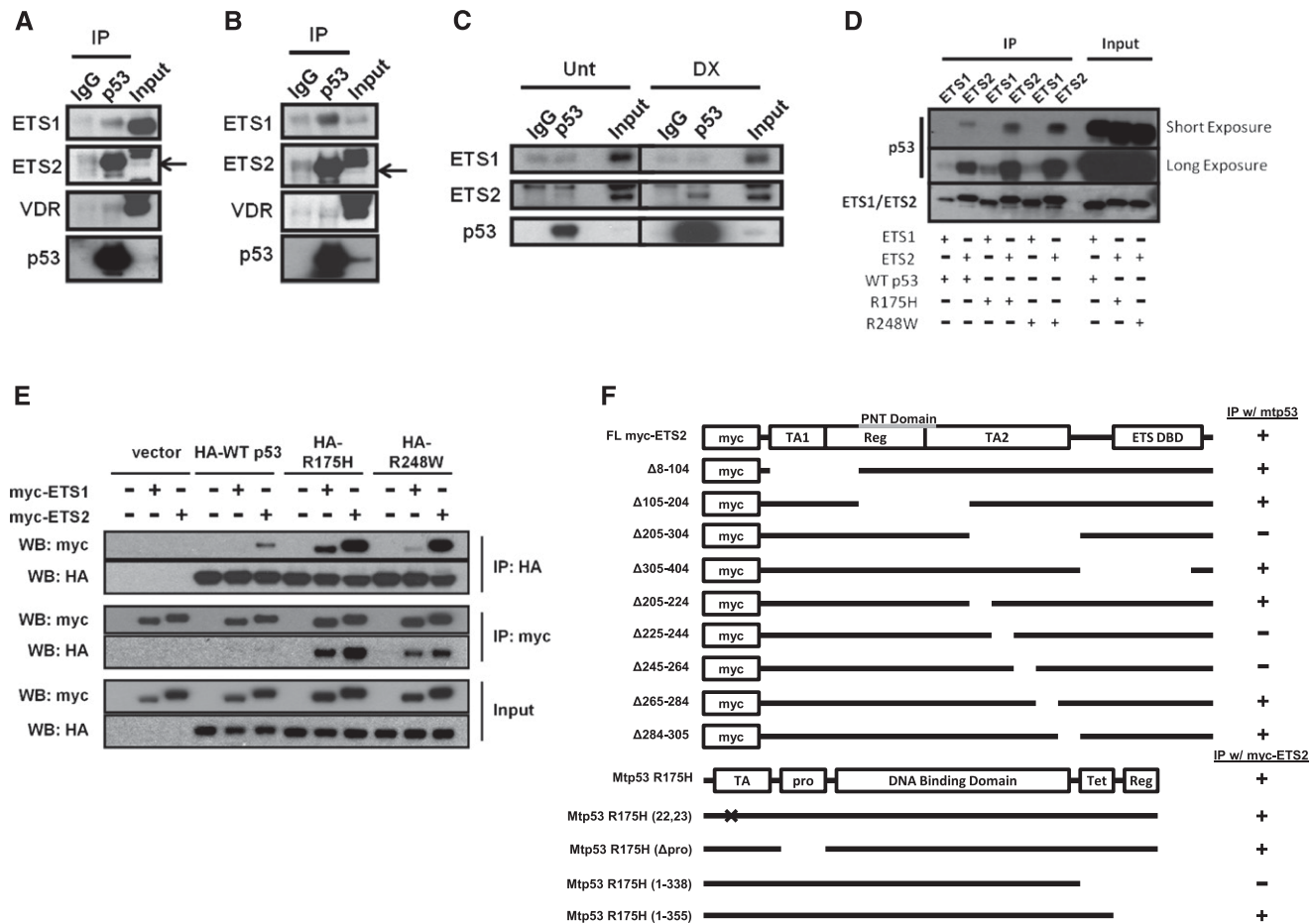


Figure 3. Interaction study of mtp53 and ETS proteins. Endogenous mtp53 can coimmunoprecipitate with ETS1 and ETS2 in MDAH087 (A) or MIA PaCa-2 (B) cell lysates. Cell lysates were immunoprecipitated using monoclonal antibodies for mtp53 and Western blot for ETS1, ETS2, and VDR using polyclonal antibodies. (C) Endogenous wild-type (WT) p53 can also interact with ETS2 in U2OS cells. U2OS cells were untreated (Unt) or treated with doxorubicin (DX) at a final concentration of 1 μ g/mL for 6 h prior to harvesting for immunoprecipitation. Lysate were then immunoprecipitated using monoclonal antibodies against mtp53 and Western blot for ETS1, ETS2, and p53 using polyclonal antibodies. (D) In vitro interaction studies using recombinant wild-type p53, mtp53 R175H, mtp53 R248W, ETS1, and ETS2. Proteins were mixed in equal proportions and immunoprecipitated with either ETS1 or ETS2 antibodies. (E) Interaction of p53 with ETS1 and ETS2. H1299 cells were cotransfected with HA-tagged p53 (wild type or mutants) and myc-tagged ETS1 or ETS2 and coimmunoprecipitated with antibodies against HA or myc tags. (F) Schematic diagram demonstrating the localization of mtp53 and ETS2 protein–protein interaction regions. H1299 cells were transfected with plasmid DNA encoding the indicated protein/protein deletions. Lysates were coimmunoprecipitated with antibodies against p53 or Myc tag. (TA1) Transactivation domain 1; (Reg) regulatory domain; (TA2) transactivation domain 2; (ETS DBD) ETS DNA-binding domain; (TA) transactivation domain; (pro) proline-rich region; (Tet) tetramerization domain.

proteins with either recombinant ETS1 or ETS2 and then performed an immunoprecipitation for the ETS proteins. Western blot analysis supported a direct association between these proteins. It also supported the observation that mtp53 bound preferentially to ETS2, as indicated by the increased level of mtp53 in the ETS2 immunoprecipitation (Fig. 3D). mtp53 also associated with ETS1; however, this was only evident in longer film exposures (Fig. 3D). Interestingly, we observed that wild-type p53 also bound ETS2, albeit to a lesser extent than the mtp53 proteins that we tested (R175H and R248W) (Fig. 3D). We obtained similar results using tagged versions of the ETS and p53 proteins, supporting the observation that mtp53 has a higher affinity for ETS2 than for ETS1. (Fig. 3E). Thus,

mtp53 directly interacts with ETS1 and ETS2 with a preference for the latter. Next, we mapped the regions involved in the interaction between mtp53 and ETS2. H1299 were transfected with myc-tagged ETS2 constructs and mtp53 and then processed for immunoprecipitation with an anti-myc tag antibody. The myc-tagged ETS2 deletion mutants lacking amino acids 8–104, 105–204, and 305–404 coprecipitated mtp53 (Fig. 3F; Supplemental Fig. S4D). Deletion of amino acids 205–304 of ETS2, which corresponds to its second transactivation domain, eliminated the interaction with mtp53 (Fig. 3F; Supplemental Fig. S4d). Smaller deletions spanning the 205–304 regions narrowed the mtp53 interaction site on ETS2 to amino acids 225–264 (Fig. 3F; Supplemental Fig. S4F). mtp53 carrying a deletion

of its proline-rich domain or double mutations in the transactivation domain (mutant 22, 23) retained the ability to interact with ETS2, as did a mtp53 deletion mutant lacking amino acids 356–393 (referred to as mutant 1-355). In contrast, the deletion mutant lacking amino acids 339–393 (referred to as mutant 1-338) lost the ability to bind ETS2 (Fig. 3F; Supplemental Fig. S4D). We also observed that the interaction between wild-type p53 and ETS2 is dependent on the same region (Supplemental Fig. 4E). Since the difference between mutant 1-355 and mutant 1-338 is that the latter lacks amino acids 339–354, we inferred that this small portion of mtp53 is required for the interaction with ETS2.

Mtp53 cooperates with ETS2 to activate TDP2 expression

Since our intention was to identify genes involved in the DNA damage response, we functionally annotated the mtp53 target genes using DAVID (Database for Annotation, Visualization, and Integrated Discovery) (Huang et al. 2009) and found that among the 602 promoters that overlapped from the ChIP-on-chip and ChIP-seq data sets, only 17 (5.63%) had established roles in the DNA damage response (Supplemental Table S5). We manually curated this set of 17 genes and found TDP2, a gene that has a unique and apparently nonredundant role in the repair of etoposide-induced DNA damage (Supplemental Table S5). TDP2 was initially identified as a protein that associates with the TNF receptor and has recently been shown to have 5'-tyrosyl DNA phosphodiesterase activity that is required for the repair of etoposide-induced DNA double-strand breaks (Pype et al. 2000; Cortes Ledesma et al. 2009; Li et al. 2011b; Zeng et al. 2011). Given that mtp53 can promote etoposide resistance, we speculated that TDP2 may represent a transcriptional target of mtp53 that contributes to chemotherapy resistance.

If the ETS proteins cooperate with mtp53 to regulate TDP2 expression, the protein complexes should be present on its promoter, and thus we used ChIP to determine whether this was the case. The TDP2 promoter has two putative ETS sites within the ChIP-seq-predicted mtp53-bound region (Fig. 4A). We determined that both mtp53 and ETS2—and to a lesser extent, ETS1—bound within the mtp53-binding sites in MDAH087 cells (Fig. 4B). The other transcription factors that we tested (PU.1, VDR, E2F1, and p63) were not significantly enriched over the IgG level (Fig. 4B). Therefore, the findings that mtp53 and ETS2 together occupy this mtp53-binding site and that there is a direct interaction between the two support the possibility that they cooperatively regulate the expression of this mtp53 target gene.

In our initial analysis (Fig. 1C,D), we observed that mtp53 knockdown reduced the level of TDP2 expression. To determine whether this decrease in mRNA levels correlated with a decrease in protein levels, we performed Western blot analysis. Consistent with our observations using qPCR, we observed that siRNA knockdown of mtp53 resulted in a decreased expression of TDP2 (Fig. 4C,D). The fact that two different siRNAs yielded the same effect (i.e.,

TDP2 down-regulation) indicated that this was not an off-target effect (Fig. 4C,D). These observations were reproducible in both MDAH087 and MIA PaCa-2 cells (Fig. 4C,D, respectively). The knockdown of wild-type p53 in U2OS, WI-38, and A549 cells did not affect TDP2 protein levels (Fig. 4E), suggesting a gain-of-function role of mtp53. To test whether the regulation of TDP2 by mtp53 was dependent on either the cell type or a particular mtp53, we screened a panel of breast and lung cancer cell lines that carry different p53 mutations. We observed that siRNA knockdown of mtp53 reduced TDP2 expression in the majority of the cell lines tested (Fig. 4F). TDP2 levels were not detectable in the HCC1171 cell line, and thus we were unable to determine whether mtp53 controlled its expression. As expected, transfection of the p53 siRNA into the p53-null H1299 cell line had no impact on TDP2 levels, further eliminating the possibility of off-target effects of these siRNAs.

One would predict that knocking down the ETS protein that recruits mtp53 to the promoter should also reduce TDP2 expression. Thus, we assessed whether ETS1 or ETS2 knockdown recapitulated the effect of mtp53 knockdown. We observed that siRNA knockdown of ETS2 resulted in reduced expression of TDP2 in both MDAH087 (Fig. 4G) and MIA PaCa-2 cells (Fig. 4H), whereas ETS1 knockdown also reduced, albeit to a lesser extent, TDP2 expression only in MDAH087 cells (Fig. 4G). Although we do not know the basis of the different response to ETS1 knockdown in these two cell lines, it is possible that it reflects tissue-specific functions of these ETS proteins. Previous studies have indicated that other transcription factors (VDR, p63, E2F1, and NF-Y) play a role in the regulation of gene expression by mtp53 (Di Agostino et al. 2006; Adorno et al. 2009; Fontemaggi et al. 2009; Stambolsky et al. 2010). In agreement with their lack of appreciable association with the TDP2 promoter in vivo (Fig. 4B), we did not observe any changes in TDP2 expression after VDR, p63, E2F1, or NF-Y knockdown, indicating that they do not regulate its expression (data not shown). The fact that mtp53 exhibits higher affinity for ETS2 both in vitro and in vivo and that ETS2 knockdown recapitulates the effect of mtp53 knockdown on TDP2 expression in both cell lines indicates that ETS2 plays a more prominent role in the regulation of this gene target by mtp53.

The change in TDP2 protein level in both cell lines corresponds to the change in relative mRNA levels (Supplemental Fig. S5A,B). It is interesting to note that mtp53 knockdown in both cell lines also reduced ETS2 protein levels (Fig. 4G,H; Supplemental Fig. S5A,B). However, the magnitude of the change in protein levels did not correspond to the change in mRNA levels, which we interpreted to suggest that mtp53 might regulate ETS2 stability (Fig. 4G,H; Supplemental Fig. S5A,B). A similar correlation between mtp53 and ETS2 protein levels was observed in some samples among the panel of breast and lung cancer cell lines (Fig. 4F). Interestingly, the H2106 lung cancer cell line, which also carries the R248W mtp53, showed the largest decrease of ETS2 protein levels upon mtp53 knockdown (Fig. 4F). To test whether mtp53 can regulate the stability of the ETS2 protein, we trans-

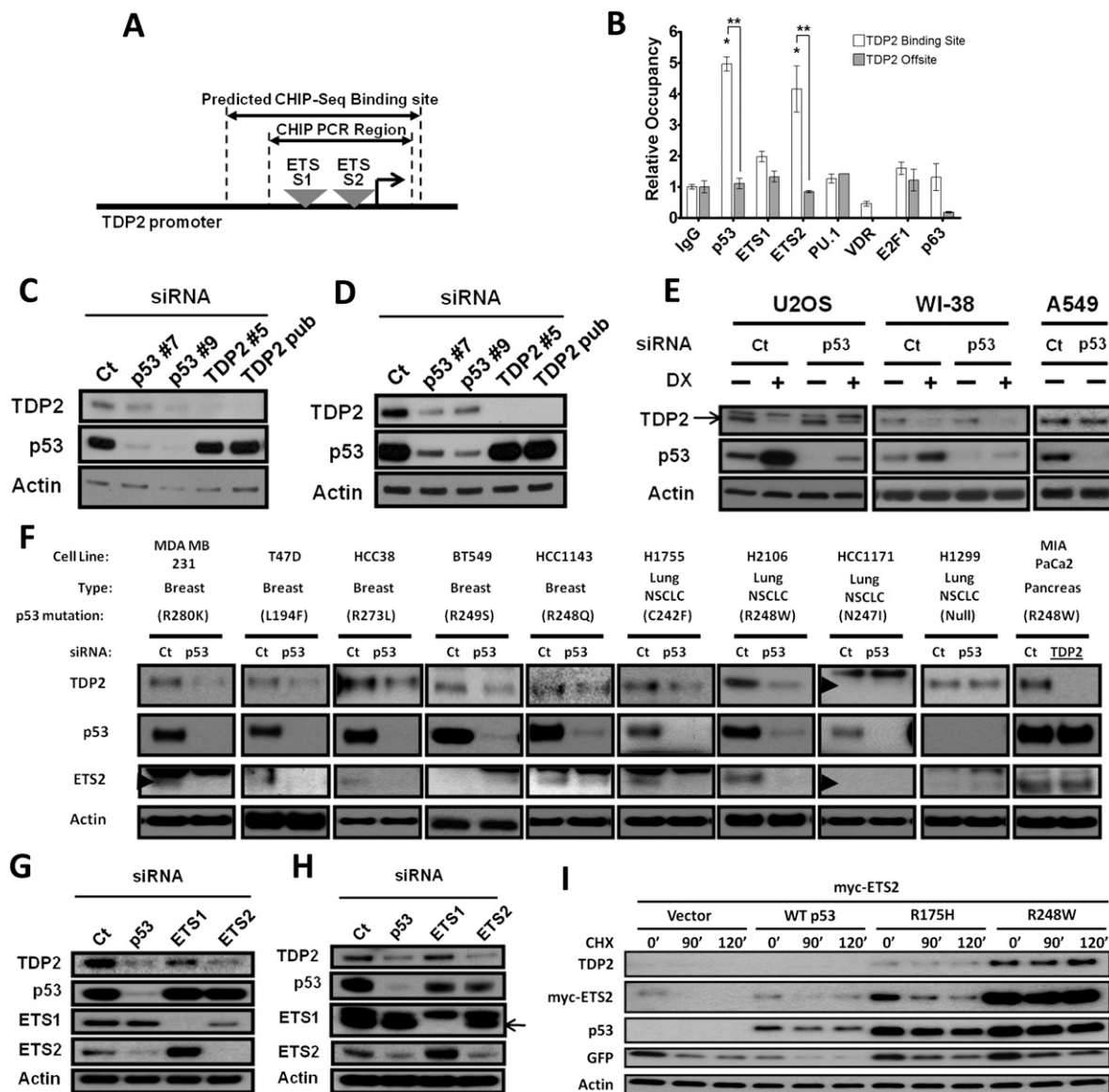


Figure 4. mtp53 cooperates with ETS2 to activate TDP2 expression. (A) Schematic of TDP2 promoter. The ChIP-seq-predicted binding site is represented by the arrow and spans from base -123 to base $+58$ relative to the TSS. MEME predicted two putative EBSs, S1 and S2, located at base -59 and base -10 , respectively. Primers were designed to amplify regions -77 to $+36$ for ChIP analysis. (B) ChIP analysis of mtp53 and ETS2 association with this region in MDAH087 cells. ChIP was performed using antibodies against p53, ETS1, ETS2, and previously reported mtp53-binding partners as indicated. The qPCR data for the specific antibody immunoprecipitations are relative to nonspecific control IgG antibodies. Primers were designed to detect the predicted binding site and an offsite 2 kb stream of the binding site (mean \pm SEM; [*] P -value ≤ 0.05 vs. IgG ChIP; [**] P -value ≤ 0.05 binding site vs. offsite). Western blot of TDP2 protein levels after different p53 and TDP2 siRNA knockdown in MDAH087 (C) and MIA PaCa-2 (D) cells. (E) Knockdown of wild-type (WT) p53 does not affect TDP2 protein levels. U2OS and WI-38 cells were transfected with either control (Ct) or p53 siRNA and then treated or untreated with doxorubicin (DX). A549 cells were transfected with control and p53 siRNA but were not treated with doxorubicin. The arrow indicates the TDP2 protein band. (F) Effect of mtp53 knockdown on TDP2 expression in various cell lines. A panel of breast and lung cancer cell lines was transfected with either control or p53 siRNA. MIA PaCa-2 cells transfected with TDP2 siRNA were included as a positive control for TDP2 detection (indicated by arrowhead). HCC1171 appears not to express TDP2. Knockdown of mtp53 and ETS2 reduces TDP2 protein levels in MDAH087 (G) and MIA PaCa-2 (H) cells. The arrow indicates ETS1 protein in MIA PaCa-2 lysates. (I) Ectopic coexpression of mtp53 and ETS2 may increase TDP2 expression in p53-null Saos2 cells by stabilizing ETS2. Saos2 cells were transfected with plasmid DNA expressing myc-ETS2 with different p53 constructs. Cells were treated with 100 ng/mL cycloheximide (CHX) for the indicated time prior to harvesting for Western blot.

fected p53-null Saos2 cells with myc-ETS2 and different p53 expression vectors. We treated the cells with cycloheximide and harvested at different time points and assessed ETS2 protein levels by Western blot. Consistent with the possibility that mtp53 can stabilize ETS2, we observed that relative to cells transfected with ETS2 alone, cells cotransfected with mtp53 and ETS2 had elevated ETS2 protein levels (Fig. 4I). The cells cotransfected with ETS2 and the R248W mutant exhibited the highest levels of ETS2 protein levels, which is likely due to the increased stability of ETS2 (Fig. 4I). The ability of mtp53 to stabilize ETS2 is specific to this protein, since we did not observe the same effect on the ETS1 protein (Supplemental Fig. S5C). These results are consistent with the observation that mtp53 knockdown did not alter ETS1 protein levels. We also observed that cotransfection of mtp53 with ETS2 reduced the level of ETS2 ubiquitination, suggesting that mtp53 may stabilize ETS2 by preventing its ubiquitin-dependent proteasomal degradation (Supplemental Fig. S5D). Importantly, we observed that the transcriptional cooperation between ETS2 and mtp53 could be reconstituted, as indicated by the fact that cells cotransfected with mtp53 and ETS2 had elevated TDP2 levels (Fig. 4I). Taken together, these data indicate that mtp53 can increase the stability of the ETS2 protein and that mtp53/ETS2 cooperate to induce TDP2 expression.

To determine whether mtp53 might also increase TDP2 levels at the post-translational level, we assessed whether knocking down mtp53 affected the protein's turnover. The knockdown of mtp53 decreased the apparent half-life of TDP2 by ~40 min (from 182.0 min \pm 4.2 min to 141.3 min \pm 0.5 min when compared with control siRNA) (Supplemental Fig. S5E,F). The difference in protein stability in conjunction with reduced transcript level likely accounts for the decrease in TDP2 protein levels in response to p53 knockdown.

To test directly whether the EBSs were involved in the regulation of TDP2 by mtp53 and the ETS proteins, we cloned the promoter (–1000 to +50 relative to the transcription start site [TSS]) into a luciferase reporter construct and also generated variants (referred to as S1 and S2) in which we individually mutated the ETS sites (GGAAG to AAAAA) (Fig. 4A). We transfected MIA PaCa-2 cells with these promoter constructs along with a control, p53, ETS1, or ETS2 siRNA and then assayed promoter activity. siRNA knockdown of mtp53 reduced the TDP2 promoter activity by ~30% (Fig. 5A). Knockdown of ETS1 and ETS2 also reduced the activity of the TDP2 promoter to the same extent (Fig. 5A). Mutation of the first ETS site (S1) reduced the activity of the promoter by ~50% and, importantly, rendered the promoter unresponsive to the knockdown of mtp53 and ETS2 (Fig. 5A). In contrast, mutation of the second ETS site (S2) reduced the overall activity of the promoter to a lesser extent than the S1 mutation and still proportionally responded to the siRNA knockdown of these proteins. Simultaneously knocking down mtp53 and ETS1 or ETS2 did not significantly reduce TDP2 promoter activity more than mtp53 knockdown alone (Supplemental Fig. S6A). We concluded that endoge-

nous mtp53, ETS1, and ETS2 can regulate expression of the cloned TDP2 promoter and that this is primarily mediated through the first ETS site (S1) in the promoter.

To further validate this observation, we tested the ability of mtp53 R175H, p63, p73, and several R175H mutant constructs to activate the TDP2 promoter in a p53-null background. The R175H mutant increased the TDP2 promoter activity by ~50% (Fig. 5B). We also observed that p63 and p73 had no effect on the TDP2 promoter (Fig. 5B). R175H mutants lacking the proline-rich domain or carrying mutations in the transactivation domain were also able to efficiently activate the TDP2 promoter (Fig. 5B). Deletion of the C-terminal 38 amino acids (mutant 1-355) modestly decreased the capacity of the mutant protein to activate the promoter. The deletion mutant lacking the C-terminal 55 amino acids (mutant 1-338) lost the ability to activate the promoter (Fig. 5B). The observation that this mutant is unable to activate the promoter is consistent with the observation that it does not interact with ETS2 (Fig. 3F).

We wanted to determine whether mtp53 and ETS proteins could cooperate in the activation of the TDP2 promoter, and thus we titrated the amounts of plasmid required to observe an effect. Interestingly, when mtp53 was transfected at lower amounts or when ETS1 or ETS2 was transfected alone, we did not observe activation of the TDP2 promoter (Fig. 5C). In contrast, cotransfection of low amounts of mtp53 with either ETS1 or ETS2 stimulated the promoter activity. We noted that different amounts of ETS1 and ETS2 were required for the cooperative activation of the TDP2 promoter, which might be due to the fact that they exhibit differences in their expression levels (data not shown). Although the activation was modest, we observed that mutation of the first ETS site (S1) eliminated the ability of these ectopically expressed proteins to activate the promoter (Fig. 5C). By titrating R248W mtp53 and ETS levels, we were able to observe an ~75% increase in TDP2 promoter activity (Fig. 5D). Taken together, these results can be interpreted to indicate that mtp53, in cooperation with either ETS1 or ETS2, can transcriptionally regulate TDP2 expression.

The data above suggest that mtp53 regulates the TDP2 promoter in a sequence-specific manner. If this is the case, then it follows that mutation of the ETS site should abrogate the binding of mtp53. To test this possibility, we generated biotin-labeled double-stranded oligonucleotides that correspond to the DNA sequences flanking the EBS in the TDP2 promoter. We included 15 bases upstream of and downstream from the ETS S1 site and additionally generated oligonucleotides in which the ETS S1 site was mutated (GGAAG to AAAAA). Nuclear extracts from MIA PaCa-2 cells were mixed with the oligonucleotides, and then the oligonucleotides (and associated proteins) were isolated with streptavidin agarose. We performed Western blot analysis to assess the binding of ETS1, ETS2, and mtp53 proteins to these oligonucleotides. We observed that ETS1 and, to a higher extent, ETS2 and mtp53 bound the wild-type oligonucleotide and that mutation of the ETS site largely eliminated their binding (Fig. 5E). We also assessed whether wild-type p53 associ-

Do et al.

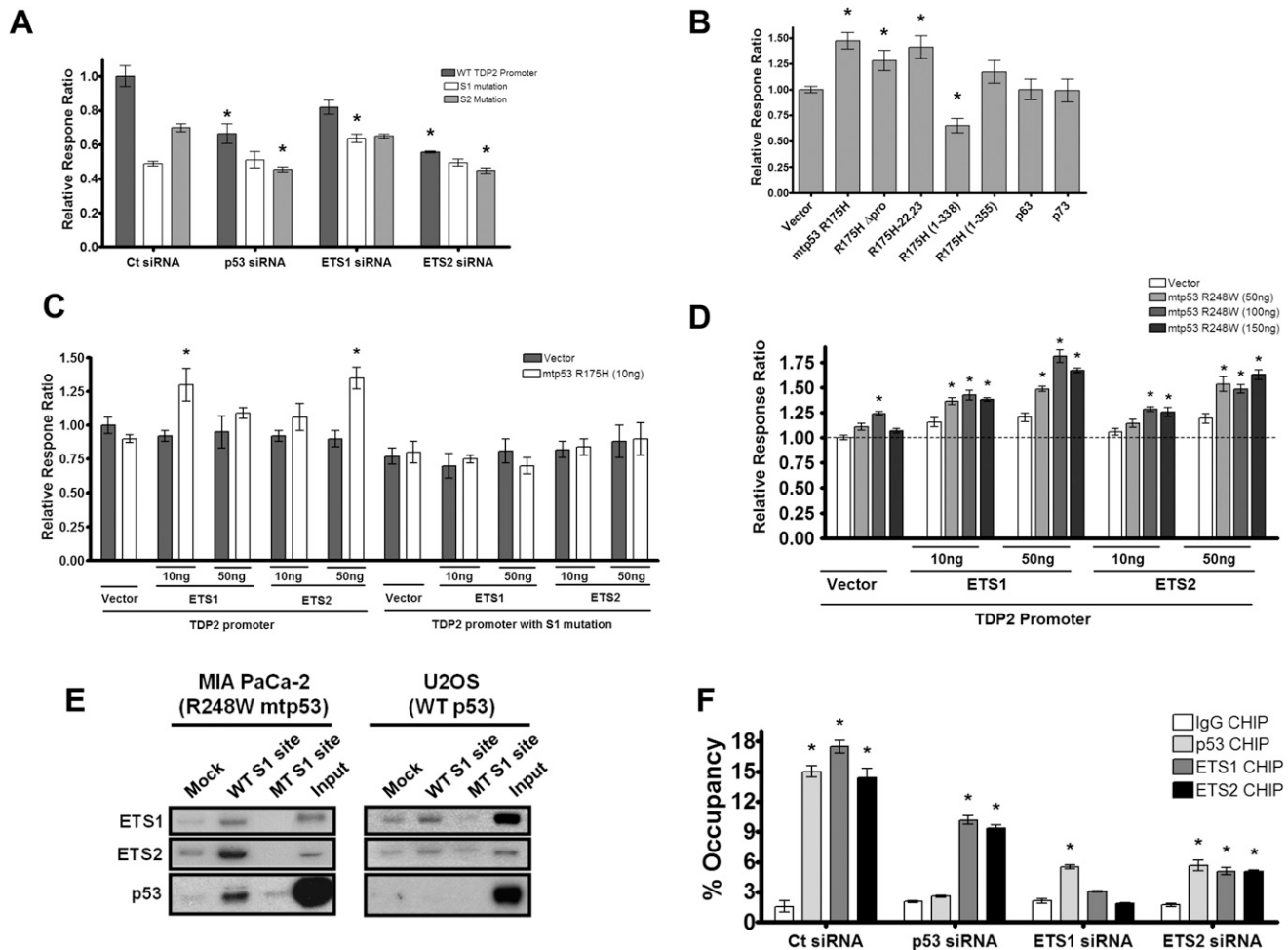


Figure 5. Functional analysis of TDP2 promoter. (A) mtp53 may coregulate the TDP2 promoter at S1. Wild-type (WT) TDP2 promoter or TDP2 promoter with point mutations in S1 or S2 converting the EBS sequence of GGAAG to AAAAA was cloned upstream of the luciferase ORF and cotransfected into MIA PaCa-2 cells with control (Ct), mtp53, ETS1, or ETS2 siRNA. Luciferase activity (relative response ratio) was normalized to *Renilla* luciferase levels (mean \pm SEM; [*] P -value ≤ 0.01 vs. control siRNA of the same promoter). (B) Ectopic expression of mtp53 in p53-null Saos2 cells increases TDP2 promoter activity. Luciferase activity in Saos2 cells cotransfected with TDP2 promoter-luciferase plasmid and 50 ng of mtp53, mtp53 deletions, or p53 family member constructs (mean \pm SEM; [*] P -value ≤ 0.05 vs. empty vector control). (C) Low levels of mtp53 R175H cooperate with ETS1 and ETS2 to activate cloned TDP2 promoter. Luciferase activity of Saos2 cells cotransfected with wild-type TDP2 promoter-luciferase plasmid or TDP2 promoter carrying mutations in S1, 10 ng of mtp53 R175H (a lower amount of p53 that does not show significant activation of TDP2 promoter), and titrating amounts of ETS1 or ETS2 DNA (mean \pm SEM; [*] P -value ≤ 0.05 vs. control siRNA of the same promoter). (D) Titration amounts of R248W mtp53 and ETS can also coactivate the TDP2 promoter. Luciferase assay was used to measure TDP2 promoter activity after cotransfection with titrating amounts of R248W mtp53 and ETS1 or ETS2 (mean \pm SEM; [*] P -value ≤ 0.01 vs. vector/vector and ETS/vector). (E) ETS1, ETS2, and mtp53 can bind to biotinylated DNA in vitro. Double-stranded biotinylated DNA containing wild-type or S1 mutant site with an addition of 15 bp upstream of and downstream from the EBS was added to MIA PaCa-2 and U2OS nuclear extracts and pulled down with streptavidin beads. No biotinylated DNA was added for “mock” pull-down. (F) mtp53 requires ETS to bind to the TDP2 promoter in MIA PaCa-2 cells. ChIP was performed using MIA PaCa-2 cells transfected with control, p53, ETS1, or ETS2 siRNA. The data are from qPCR using ChIP DNA, with antibodies indicated relative to 1.0% input (mean \pm SEM; [*] P -value ≤ 0.01 vs. IgG ChIP).

ated with this oligonucleotide using nuclear extracts from U2OS cells. Importantly, we did not detect wild-type p53 binding (Fig. 5E). Interestingly, whereas we could detect ETS1 binding in this pull-down assay, ETS2 binding was only slightly above the mock control. Taken together, our data indicate that mtp53 (and not wild-type p53) is recruited to the TDP2 promoter via an ETS site and that this site is required for the regulation of the promoter's activity by mtp53.

We then wanted to test whether mtp53's presence on the TDP2 promoter was dependent on the ETS proteins. To do so, we knocked down mtp53, ETS1, and ETS2 in MIA PaCa-2 cells and then determined the association of these proteins with the TDP2 promoter using ChIP. Control siRNA transfected cells have mtp53, ETS1, and ETS2 bound to the TDP2 promoter (Fig. 5F; Supplemental Fig. S6B). As expected, knocking down mtp53 abolished mtp53's occupancy of the TDP2 promoter and reduced

the occupancy of both ETS1 and ETS2 on the TDP2 promoter by ~50% (Fig. 5F; Supplemental Fig. S6B). Interestingly, knocking down either ETS1 or ETS2 strongly reduced the association of both mtp53 and the nontargeted ETS protein with the TDP2 promoter. Although we do not know the specific reason for these results, we speculate that the ETS proteins may associate with the TDP2 promoter in an interdependent manner (Fig. 5F). Additionally, since siRNA knockdown of either ETS1 or ETS2 resulted in decreased levels of mtp53 protein in these cells, this would conceivably impact the amount of the ETS/mtp53 proteins detected on the TDP2 promoter (Fig. 4H; Supplemental Fig. S6C).

Since we determined that ETS1 is present on the TDP2 promoter and that knockdown of ETS1 does affect TDP2 levels, we tested whether the change in TDP2 protein levels after ectopic expression of mtp53 and ETS2 was ETS1-dependent in p53-null Saos2 cells (Supplemental Fig. 6D). Interestingly, ETS1 knockdown actually increased TDP2 protein levels when the cells ectopically expressed mtp53 in both the presence and absence of ectopically expressed ETS2 (Supplemental Fig. 6D). This elevated level of TDP2 may be due to the fact that endogenous ETS2 levels also increase in response to ETS1 knockdown (Fig. 4G,H; Supplemental Figs. S5B,C, 6D).

To extend our observation that the ETS site was important for the recruitment of mtp53 to promoters, we selected 10 additional genes that overlap with the ETS1 ChIP-seq and performed qPCR on RNA extracted from MIA PaCa-2 cells transfected with control, p53, ETS1, and ETS2 siRNA (Supplemental Fig. S7). We observed that other genes such as WRAP53, THADA, DEPDC1B, and GOLGA1 also had reduced transcript levels following mtp53/ETS2 knockdown and had either no change or an increase in levels after ETS1 knockdown (Supplemental Fig. S7). We further assessed whether WRAP53 is regulated by mtp53 and ETS2 (Supplemental Fig. 8A). ChIP experiments confirmed the association of mtp53 with this promoter, and we also observed that mtp53 and ETS2 knockdown reduced WRAP53 protein levels (Supplemental Fig. S8B,C). Examination of the WRAP53 promoter revealed that the predicted mtp53-binding site also contained an EBS (GGAAA) (Supplemental Fig. S8A). We cloned a 1.15-kb fragment of the WRAP53 β promoter (−1080 to +70) and tested whether it responded to the knockdown of mtp53 and ETS2. We observed that the activity of the WRAP53 promoter decreased when we knocked down mtp53 or ETS2, and mutation of the EBS (GGAAA to AAAAA) abrogated this response (Supplemental Fig. S8D). Taken together, our data showing that mtp53 and ETS2 knockdown alter the expression of several mtp53 target genes suggest that this may be a prevalent mechanism for the regulation of gene expression by mtp53.

Regulation of etoposide resistance

The topoisomerase II poison etoposide is widely used for the treatment of cancers; however, resistance to this chemotherapy can occur. mtp53 correlates with the

acquisition of chemotherapy resistance and, when ectopically expressed, can prevent etoposide-induced apoptosis (Blandino et al. 1999). mtp53 can promote survival through multiple mechanisms, such as directly inactivating its family members (Tap63 and Tap73) and also by cooperating with other transcription factors (e.g., NF- κ B and VDR). A number of mtp53 transcriptional targets have been described, but for the most part, these genes lack enzymatic activity (Weisz et al. 2004, 2007; Zalcenstein et al. 2006; Yan et al. 2008; Yan and Chen 2009).

The observation that siRNA knockdown of mtp53 reduced TDP2 levels suggested that the up-regulation of this mtp53 target gene may contribute to chemotherapy resistance. Therefore, we tested whether siRNA knockdown of TDP2 impacted cell viability in response to etoposide treatment. TDP2 knockdown increased the sensitivity to etoposide in both MIA PaCa-2 and MDAH087 cells (Fig. 6A; Supplemental Fig. S9A). We noted that the MIA PaCa-2 cells appeared to exhibit intrinsically higher sensitivity to etoposide, which may be related to their more rapid growth rate. Nevertheless, suppression of TDP2 expression in both cell lines reduced cell viability after etoposide treatment. TDP2 knockdown did not similarly increase the sensitivity to cisplatin, a DNA-damaging agent that cross-links DNA strands. However, TDP2 knockdown did modestly increase sensitivity to doxorubicin, which induces apoptosis through topoisomerase II-dependent and -independent mechanisms (i.e., reactive oxygen species) (Supplemental Fig. S9B,C).

To determine whether this sensitization to etoposide was due to an increased level of apoptosis, we assayed caspase-3 cleavage using fluorescence-activated cell sorting (FACS) analysis and immunofluorescence microscopy (Fig. 6B,C). In cells transfected with TDP2 siRNA, we observed an increased sensitivity to etoposide, as indicated by the elevated levels of cleaved caspase-3 that was detected. The sensitization to etoposide that occurs in TDP2 knockdown cells was most evident at the lowest dose (5 μ g/mL), and the trend continued at the higher doses (Fig. 6B). Likewise, siRNA knockdown of mtp53 increased the sensitivity to etoposide (Fig. 6C). To obtain biochemical confirmation of caspase activation, we performed Western blot analysis to detect PARP cleavage, a caspase substrate that is cleaved upon activation of apoptosis (Fig. 6D). In this experiment, we transfected cells with control, p53, or TDP2 siRNA and then treated the cells with different doses of etoposide. mtp53 and TDP2 siRNAs potently suppressed TDP2 expression and increased the amount of cleaved PARP that occurred upon etoposide treatment (Fig. 6D). In this analysis, we also detected an increased sensitivity to etoposide in the cells transfected with siRNAs targeting either p53 or TDP2. Importantly, TDP2 knockdown appeared to have a greater sensitizing effect than mtp53 knockdown, despite the fact that it had no effect on mtp53 expression (Fig. 6D). This is significant because it suggests that mtp53's other prosurvival activities may not be able to override the apoptotic signals activated by the combined TDP2 knockdown and etoposide treatment. These data suggest that one of the mechanisms by which mtp53 can confer chemotherapy resistance is by up-regulating TDP2 expression.

Do et al.

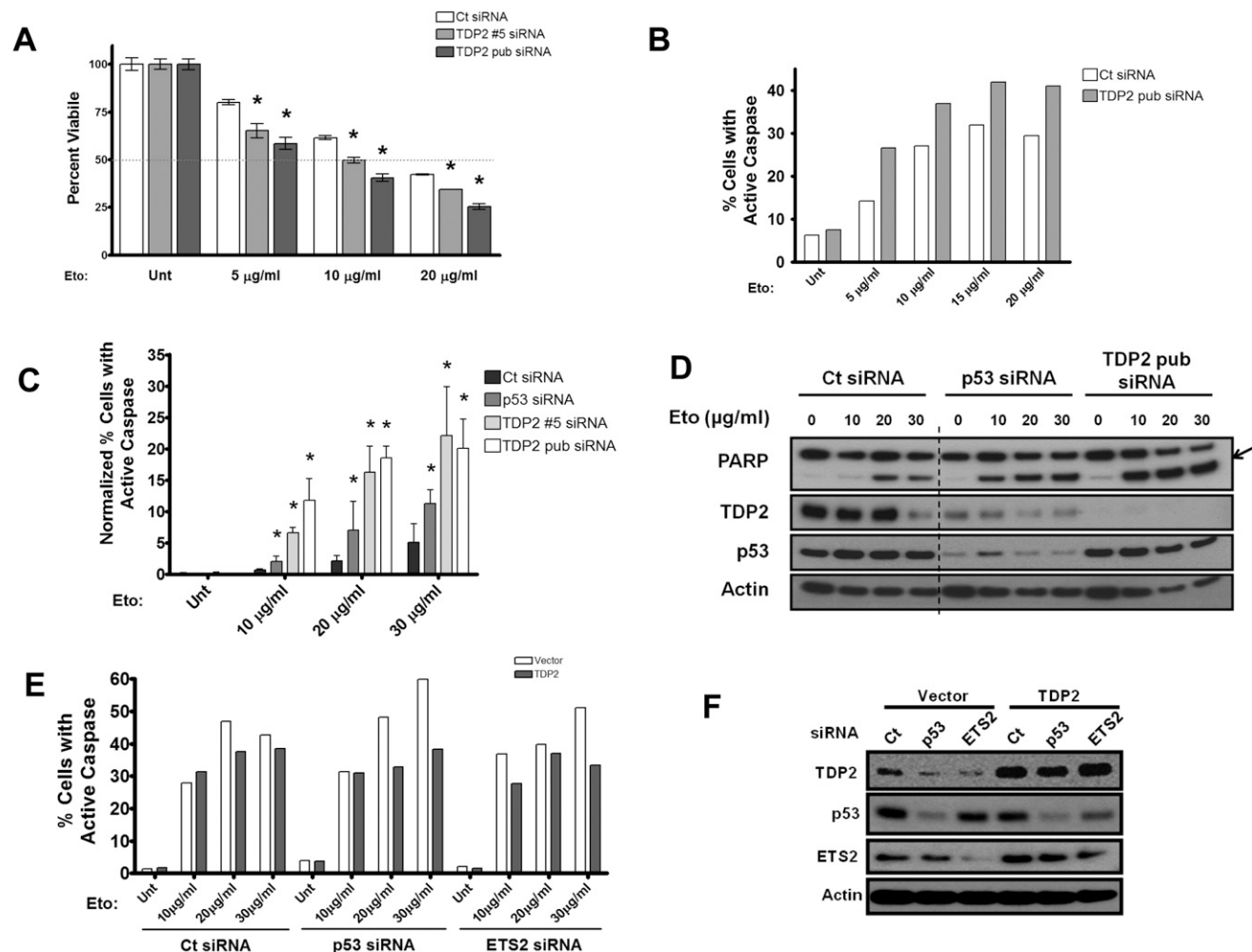


Figure 6. Reduction of TDP2 protein levels by depletion of either p53 or TDP2 sensitizes cells to etoposide. (A) MIA PaCa-2 cells were more sensitive to etoposide after TDP2 knockdown. MIA PaCa-2 cells were transfected with two different siRNAs targeting TDP2 and then treated with increasing concentrations of etoposide for 24 h. Cell viability was measured by CellTiter Blue assay (mean \pm SD; [*] P -value ≤ 0.05 vs. control [Ct] siRNA of the same Eto concentration). (B) FACS analysis revealed increased apoptosis in TDP2 knockdown MIA PaCa-2 cells. MIA PaCa-2 cells were transfected with either control or TDP2 siRNA and, 2 d later, were treated with increasing concentrations of etoposide for 48 h. Cells were stained for cleaved caspase-3 and were assayed by flow cytometry. These are the representative data of three independent experiments. (C) Knockdown of mtp53 and TDP2 increases apoptosis when treated with etoposide. MIA PaCa-2 cells transfected with p53 or different TDP2 siRNAs were treated with increasing concentrations of etoposide for 24 h. Cells were analyzed by immunofluorescence microscopy to detect DAPI and cleaved caspase-3. Data represent caspase-3-positive cells normalized to untreated cells (mean \pm SD; [*] P -value ≤ 0.05 vs. control siRNA of the same Eto concentration). (D) Western blot of MIA PaCa-2 cells transfected with different siRNAs and treated with 0, 10, 20, or 30 μ g/mL etoposide for 48 h. Arrow represents cleaved PARP, which is an indicator of increased caspase activity and apoptosis. Intervening lanes are spliced out where indicated, but all siRNA and drug treatments represent data from the same immunoblot with the same exposure. (E) Ectopic expression of TDP2 rescues etoposide sensitivity in mtp53 and ETS2 knockdown MIA PaCa-2 cells. MIA PaCa-2 cells stably expressing TDP2 or empty vector were transfected with control, p53, or ETS2 siRNA. Cells were then treated with increasing concentrations of etoposide. Caspase-positive cells were assayed by flow cytometry. These data are representative of four independent experiments. (F) Western blot of untreated cells used in flow cytometric analysis confirmed that the ectopic expression of TDP2 is not affected by mtp53 or ETS2 knockdown.

It follows from our studies above that if TDP2 is an important downstream component of mtp53's ability to promote etoposide resistance, then complementing its expression should reduce the sensitization effect of knocking down mtp53. We used the MIA PaCa-2 cells to generate polyclonal stable cell lines with either an empty vector or a vector expressing TDP2 and then determined the sensitivity of these different cell lines to the combina-

tion of mtp53 or ETS2 knockdowns and etoposide treatment (Fig. 6E). As expected, knockdown of mtp53 increased the sensitivity to etoposide, as determined by the increased level of active caspase-3 (Fig. 6E). In contrast, cells that ectopically expressed TDP2 exhibited comparatively less sensitivity to etoposide, even though the levels of mtp53 were greatly reduced by siRNA knockdown (Fig. 6E,F). Furthermore, we observed that ETS2 knockdown also in-

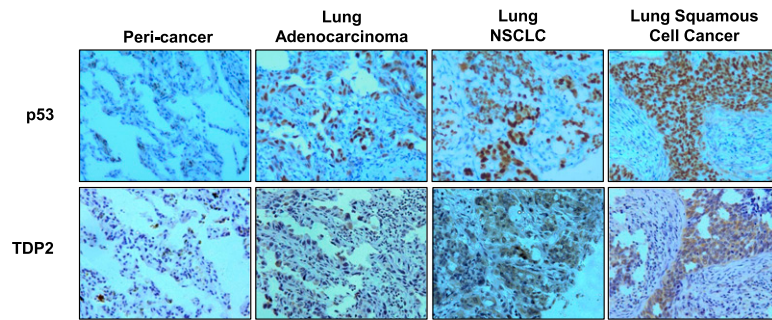


Figure 7. Immunohistochemical staining of p53 and TDP2 in lung cancer or peri-cancer tissues. The representative staining images of a TMA stained with anti-EAPII and anti-p53 antibodies.

creased the sensitivity to etoposide, and as was the case with mtp53 knockdown, ectopically expressed TDP2 attenuated the sensitivity of these cells to etoposide. Collectively, our data indicate that TDP2 is an important component of mtp53's gain-of-function activities because it can confer resistance to etoposide.

Correlation between mtp53 and TDP2 overexpression in lung cancer

To ascertain whether our in vitro observations were reflected in an in vivo setting, we immunohistochemically stained a lung cancer tissue microarray (TMA) containing 65 cases of lung cancer tissues and 32 cases of adjacent nonneoplastic tissue for p53 and TDP2. The wild-type p53 protein is typically not detectable by immunohistochemistry, whereas the mutant protein is overexpressed due to its increased stability. As expected, none of the normal lung tissue exhibited any p53 staining (Fig. 7). The majority of the cancer tissues (58.5%) stained double positive for both p53 and TDP2, while only 7.7% of the cancer tissues that had p53 overexpression did not have elevated TDP2 levels (Table 2). It is interesting to note that of the cancer tissues stained positive for p53 ($n = 43$), 88.4% of these tissues also over express TDP2, and of the cancer tissues positive for TDP2 ($n = 57$), 66.8% also stained positive for p53. No normal tissues stained double positive for both p53 and TDP2. We also observed that TDP2 expression was elevated in some normal and lung cancer tissue that did not exhibit p53 overexpression. We speculate that in these cases, TDP2 expression is elevated through an alternative mechanism. All together, these results suggest that TDP2 overexpression correlates with mtp53 in human lung cancer.

Discussion

Mutations in the p53 gene can compromise its ability to transcriptionally regulate genes that mediate its tumor suppressor activity. These mutant proteins have been shown to be potent oncogenes that have the ability to confer different oncogenic phenotypes, including resistance to apoptotic stimuli, promotion of angiogenesis, and metastasis. In this study, we present evidence that mtp53 associates with a large number of promoters that carry EBSs. Moreover, we demonstrate that mtp53 can directly interact with the ETS2 protein and that the complex formed by these two transcription factors regulates TDP2 expression transcriptionally in a sequence-specific manner. We found that many of the mtp53 target genes that were identified through our ChIP-on-chip and ChIP-seq analyses of promoter regions contain ETS sites. The ETS site is 5 bases long and thus has a high probability of occurrence in any segment of the genome. However, we observed that the ETS sites identified in these target genes were essentially within the predicted mtp53-binding site. The finding that the ETS site is abundant in many of these genes raises the possibility that the mtp53/ETS2 complex may be involved in the regulation of several of mtp53's gain-of-function activities.

Overall, our data support a role for ETS2 in cooperating with mtp53 in the regulation of various genes containing EBSs in their promoters. However, we cannot exclude the possibility that other ETS family members also interact with the mtp53/ETS2 complex and regulate the activity of this complex. Alternatively, other ETS family members might form independent complexes with mtp53. Indeed, ETS1 can also interact with mtp53, and knockdown of ETS1 reduced TDP2 expression (in MDAH087) (Fig. 4G; Supplemental Fig. S5A) and the recruitment of mtp53 and

Table 2. Majority of lung carcinoma overexpress p53 and TDP2

Tissue type (n)	p53 ⁺ TDP2 ⁺	p53 [−] TDP2 [−]	p53 ⁺ TDP2 [−]	p53 [−] TDP2 ⁺	<i>P</i> -value ^a	<i>P</i> -value ^b
Normal lung tissue ($n = 32$)	0 (0.0%)	22 (68.8%)	1 (3.1%)	9 (28.1%)		
Lung cancer ($n = 65$)	38 (58.5%)	3 (4.6%)	5 (7.7%)	19 (29.2%)	0.022	0.000

Lung cancer TMAs containing 65 cases of lung cancer and 32 cases of adjacent nonneoplastic tissues were immunohistochemically stained for p53 and TDP2. p53 and TDP2 staining was accordingly scored as either negative staining (<10% staining) or positive staining ($\geq 10\%$ staining).

χ^2 test and Fisher's exact test.

^a*P*-value: p53⁺ and TDP2⁺ versus p53[−] TDP2⁺ and p53⁺ TDP2[−].

^b*P*-value: p53⁺ and TDP2⁺ of the cancer group versus p53[−] and TDP2[−] in the pericancer tissue.

ETS2 to the TDP2 promoter (MIA PaCa-2) (Fig. 5F; Supplemental Fig. S6B). Additionally, some of the mtp53 target genes (e.g., NKIRAS1, TAF12, and DHX8) respond to mtp53 knockdown, but not to ETS1 or ETS2 knockdown (Supplemental Fig. S7). Since the promoters of these genes contain EBSs and they have been described as ETS target genes (Hollenhorst et al. 2009), we can only speculate that mtp53 might be recruited to these genes via interactions with other ETS family members or through a distinct mechanism. Further studies are required to determine how ETS1 affects mtp53's transcriptional regulatory activity and to determine whether mtp53 also cooperates with other ETS family members to regulate gene expression.

It is worth pointing out that despite the fact that we detected a weak interaction between ETS2 and wild-type p53 (Fig. 3C–E), knockdown of the latter did not affect TDP2 expression in either normal or cancer cells (Fig. 4E). It is important to note that wild-type p53 interacts with ETS2 within the same domain as mtp53 (Supplemental Fig. S4D,E). We speculate that mutations in the DNA-binding domain may cause conformational changes that could alter mtp53's affinity to ETS proteins. In addition, a previous study has suggested that other cofactors (e.g., CBP) are required for the formation of functional ETS1 and wild-type p53 complexes (Xu et al. 2002). Thus, a comparison of ETS complexes containing either wild-type p53 or mtp53 may provide insight into the differences in regulation of gene expression.

We demonstrated that mtp53 regulates the expression of the TDP2 gene, which encodes a protein that has 5'-tyrosyl DNA phosphodiesterase activity that is required for the repair of etoposide-induced DNA double-strand breaks (Cortes Ledesma et al. 2009; Adhikari et al. 2011; Zeng et al. 2011). The identification of TDP2 as a mtp53 target is important because it reveals an enzymatic activity that can be targeted to sensitize cells that express mtp53. Importantly, siRNA knockdown of TDP2 had no effect on mtp53 expression, yet was able to sensitize cells to etoposide. These data suggest that targeting TDP2 may circumvent the various anti-apoptotic activities of mtp53.

TDP2 was initially identified as a protein (referred to as TTRAP) that associates with CD40, the tumor necrosis factor (TNF) receptor 75, and several TNF receptor-associated factors (TRAFs) (Pype et al. 2000). In those studies, TDP2 (TTRAP) inhibited the activation of NF- κ B by some, but not all, stimuli (Pype et al. 2000). TDP2 (TTRAP) has also been shown to be involved in the TGF β pathway via an interaction with Smad3 and to have a proapoptotic function when associated with Parkinson's disease-associated DJ-1 mutant proteins (Esguerra et al. 2007; Adorno et al. 2009; Zucchelli et al. 2009). Intriguingly, TDP2 (referred to as EAPII) was also shown to interact with and inhibit ETS1's transactivation activity (Pei et al. 2003). However, contrary to expectations, ectopically expressed TDP2 does not have a growth inhibitory effect (Pei et al. 2003; Li et al. 2011a). In fact, it was reported recently that TDP2 (EAPII) can promote cell growth and survival of human cancer cell lines (Li et al. 2011a). Furthermore, TDP2 (EAPII) expression was found to be elevated in the majority of non-small-cell lung cancer

(NSCLC) cases (Li et al. 2011a). Importantly, mutations in the p53 gene occur in ~50% of NSCLCs, and p53 mutations have been reported to correlate with resistance to neo-adjuvant chemotherapy involving cisplatin, etoposide, and radiotherapy (Takahashi et al. 1989; Tseng et al. 1999; Wistuba et al. 2001; Yan et al. 2009). Our analysis of lung cancer tissue supports the notion that mtp53 may drive chemotherapy resistance in human cancer through the transcriptional up-regulation of TDP2.

Materials and methods

Primers and strains

All plasmids were constructed, transformed, and carried in *Escherichia coli* strain TOP10 (Invitrogen). Oligos (including siRNA sequences) used in this study are listed in Supplemental Table S1.

Antibodies, ChIP, immunoprecipitation, biotin pull-down, and Western blot

All antibodies were obtained from Santa Cruz Biotechnology, Inc., unless otherwise noted. ChIP was performed using EZ-ChIP protocol (Millipore) using 5 μ g of antibodies (IgG, sc-2027 or sc-2025; p53 FL-393, sc-6243; ETS1, sc-350; ETS2, sc-351; PU.1, sc-352; VDR, sc-1008; E2F1, sc-193; and p63, sc-8431) per reaction. Ectopic expression of mtp53 and ETS2 (for coimmunoprecipitation) was performed by cotransfecting H1299 cells with different p53 constructs (Strano et al. 2002) with full-length pCMV-myc-ETS2 or series myc-ETS2 with various 100- or 20-amino-acid deletions. Lysates were coimmunoprecipitated with myc or HA antibodies (Abcam, ab9123 or ab9110, respectively).

Reconstitution of TDP2 activation and ETS2 stability was performed in Saos2 cells. Myc-ETS2, p53 constructs, and pEGFP-C2 were transfected into Saos2 at a ratio of 1:3:0.5. Final concentration of 100 ng/mL cycloheximide was added to growth medium at 90 and 120 min prior to harvesting to stop protein synthesis.

Recombinant protein was synthesized using the PURExpress In Vitro Protein Synthesis kit (New England Biolabs). The ORFs encoding p53 (wild type and mutants), ETS1, and ETS2 were PCR-amplified with T7 promoter, generated by primer extensions, and added to the kit-provided T7 transcriptional and translation machinery, as indicated by the manufacturer's protocol, in 10- μ L reactions. Equal amounts of the synthesized p53 and ETS1 or ETS2 proteins (3 μ L of each) were added to 1 mL of immunoprecipitation buffer and immunoprecipitated with ETS1 or ETS2 antibodies as previously described. The protein preparations were not purified prior to the analysis of the interactions and thus are considered partially pure because they contain the T7 polymerase and translation machinery.

For biotin pull-downs, the synthesized double-stranded biotinylated oligonucleotide CGGTGCAGAGCGGCAGGAAGATGGAGTTGGGGAGTT, consisting of the core EBS (bold letters) flanked by 15 bp of the native promoter sequence upstream of and downstream from the core site, was mixed with MIA PaCa-2 or U2OS nuclear extract and pulled down as described (Liu et al. 2001). Mutated sequences substituted the EBS GGAAG to AAAAA or GGATG.

ChIP-chip and ChIP-seq

ChIP-on-chip DNA prepared using the Farnham laboratory protocol and was sent to Nimblegen, where the library was prepared and analyzed (Weinmann et al. 2002). ChIP-on-chip data were analyzed by NimbleScan using default settings and visualized

using SignalMap software (Nimblegen). The ChIP-seq DNA library was prepped using ChIP-Seq DNA Prep kit (Illumina) and was sent to Illumina for analysis. ChIP-seq data were analyzed by CLC Genomics Workbench using default settings. Visualization of ChIP-seq peaks was performed on Illumina GenomeStudio software. Both platform data sets were mapped to the human genome build Hg18 for direct comparison. The promoter region is defined as the genomic DNA region within 5 kb upstream of and 1 kb downstream from an annotated TSS according to annotations from Nimblegen (SignalMap software). To map and compare binding sites, coordinates for peaks predicted by the above software were entered into Microsoft Excel, and formulas were written to determine the proximity to TSSs and to other peaks. Predicted peaks were aligned using Tmod software, which runs Windows (Microsoft)-based versions of MEME (Bailey and Elkan 1994; Sun et al. 2010). Discovered motifs were compared with known transcription factors (TRANSFACS and JASPAR database) using the TOMTOM motif comparison tool of the online MEME suite (Gupta et al. 2007). The Gene Expression Omnibus accession number for the data set is GSE36752.

Luciferase assay

MIA PaCa-2 and Saos2 cells were seeded into 96-well plates (Greiner-Bio) at 7000 and 10,000 cells per well, respectively. Each well seeded with MIA PaCa-2 cells was independently transfected (five replicates for each transfection) with 50 ng of pGL4.14-luc2 (with or without promoter) (Promega), 50 ng of siRNA, and 10 ng of pRL-TK (*Renilla* luciferase). Wells seeded with Saos2 cells were transfected (five replicates) with 50 ng of pGL4.14-luc2 (with or without promoter), 10 ng or 50 ng of expression vector, and 50 ng of pRL-TK. Luciferase levels were assayed using Dual-Glo luciferase assay system (Promega). The relative response ratio (RRR) was calculated as described by the Dual-Glo manual.

Cell viability and apoptosis assays

MIA PaCa-2 and MDAH087 cells were transfected with the indicated siRNA and passed into 96-well plates at 7000 per well 24 h post-transfection. Wells were treated in triplicate with different concentrations of chemotherapy drugs 48 h post-transfection for 24 h. CellTiter-Blue cell viability assay (Promega) was used to determine cell survival. Calculations were performed as described by Promega.

Apoptosis was measured by Western blot, immunofluorescence, and flow cytometry (FACS) analysis. MIA PaCa-2 cells transfected with p53 and TDP2 siRNAs were treated with 0, 10, 20, 30 μ g/mL etoposide 48 h post-transfection for 48 h, when proteins were harvested for Western blot. Immunofluorescence was performed according to the immunofluorescence general protocol (Cell Signaling Technology). FACS for assay of apoptotic cells was performed using the flow cytometry protocol (Cell Signaling Technology).

TMA

Lung cancer TMA containing 65 cases of lung cancer and 32 cases of adjacent nonneoplastic tissues was constructed by Cancer Research Institute, Xiangya School of Medicine, Central South University (Changsha, Hunan, China) and was a kind gift from Professor Songqing Fan (Central South University, Hunan, China). All samples were anonymous, and the diagnosis of normal or tumor was reconfirmed by one of us (S. Fan, pathologist). Immunohistochemical staining was performed using the streptavidin/peroxidase (S-P) method as previously described (Li et al. 2011a).

Acknowledgments

This study is supported in part by grants from the National Center for Research Resources (5P20RR016476-11), the National Institute of General Medical Sciences (8 P20 GM103476-11) from the National Institutes of Health, and a Research Scholar Grant (RSG-08-084-01) to L.A.M. from the American Cancer Society.

References

- Adhikari S, Karmahapatra SK, Elias H, Dhopeswarkar P, Scott Williams R, Byers S, Uren A, Roy R. 2011. Development of a novel assay for human tyrosyl DNA phosphodiesterase 2. *Anal Biochem* **416**: 112–116.
- Adorno M, Cordenonsi M, Montagner M, Dupont S, Wong C, Hann B, Solari A, Bobisse S, Rondina MB, Guzzardo V, et al. 2009. A Mutant-p53/Smad complex opposes p63 to empower TGF β -induced metastasis. *Cell* **137**: 87–98.
- Babayeva ND, Wilder PJ, Shiina M, Mino K, Desler M, Ogata K, Rizzino A, Tahirov TH. 2010. Structural basis of Ets1 co-operative binding to palindromic sequences on stromelysin-1 promoter DNA. *Cell Cycle* **9**: 3054–3062.
- Bailey TL, Elkan C. 1994. Fitting a mixture model by expectation maximization to discover motifs in biopolymers. *Proc Int Conf Intell Syst Mol Biol* **2**: 28–36.
- Basuyaux JP, Ferreira E, Stehelin D, Buttice G. 1997. The Ets transcription factors interact with each other and with the c-Fos/c-Jun complex via distinct protein domains in a DNA-dependent and -independent manner. *J Biol Chem* **272**: 26188–26195.
- Bergamaschi D, Gasco M, Hiller L, Sullivan A, Syed N, Trigiante G, Yulug I, Merlano M, Numico G, Comino A, et al. 2003. p53 polymorphism influences response in cancer chemotherapy via modulation of p73-dependent apoptosis. *Cancer Cell* **3**: 387–402.
- Bischoff FZ, Yim SO, Pathak S, Grant G, Siciliano MJ, Giovannella BC, Strong LC, Tainsky MA. 1990. Spontaneous abnormalities in normal fibroblasts from patients with Li-Fraumeni cancer syndrome: Aneuploidy and immortalization. *Cancer Res* **50**: 7979–7984.
- Blandino G, Levine AJ, Oren M. 1999. Mutant p53 gain of function: Differential effects of different p53 mutants on resistance of cultured cells to chemotherapy. *Oncogene* **18**: 477–485.
- Botcheva K, McCorkle SR, McCombie WR, Dunn JJ, Anderson CW. 2011. Distinct p53 genomic binding patterns in normal and cancer-derived human cells. *Cell Cycle* **10**: 4237–4249.
- Brosh R, Rotter V. 2009. When mutants gain new powers: News from the mutant p53 field. *Nat Rev Cancer* **9**: 701–713.
- Charlot C, Dubois-Pot H, Serchov T, Tourrette Y, Wasyluk B. 2010. A review of post-translational modifications and subcellular localization of Ets transcription factors: Possible connection with cancer and involvement in the hypoxic response. *Methods Mol Biol* **647**: 3–30.
- Cortes Ledesma F, El Khamisy SF, Zuma MC, Osborn K, Caldecott KW. 2009. A human 5'-tyrosyl DNA phosphodiesterase that repairs topoisomerase-mediated DNA damage. *Nature* **461**: 674–678.
- Di Agostino S, Strano S, Emiliozzi V, Zerbini V, Mottolise M, Sacchi A, Blandino G, Piaggio G. 2006. Gain of function of mutant p53: The mutant p53/NF-Y protein complex reveals an aberrant transcriptional mechanism of cell cycle regulation. *Cancer Cell* **10**: 191–202.
- Di Como CJ, Gaiddon C, Prives C. 1999. p73 function is inhibited by tumor-derived p53 mutants in mammalian cells. *Mol Cell Biol* **19**: 1438–1449.

Do et al.

- Esguerra CV, Nelles L, Vermeire L, Ibrahimi A, Crawford AD, Derua R, Janssens E, Waelkens E, Carmeliet P, Collen D, et al. 2007. Ttrap is an essential modulator of Smad3-dependent Nodal signaling during zebrafish gastrulation and left-right axis determination. *Development* **134**: 4381–4393.
- Fontemaggi G, Dell'Orso S, Trisciuglio D, Shay T, Melucci E, Fazi F, Terrenato I, Mottolise M, Muti P, Domany E, et al. 2009. The execution of the transcriptional axis mutant p53, E2F1 and ID4 promotes tumor neo-angiogenesis. *Nat Struct Mol Biol* **16**: 1086–1093.
- Fujiwara S, Fisher RJ, Bhat NK, Diaz de la Espina SM, Papas TS. 1988. A short-lived nuclear phosphoprotein encoded by the human ets-2 proto-oncogene is stabilized by activation of protein kinase C. *Mol Cell Biol* **8**: 4700–4706.
- Gaidon C, Lokshin M, Ahn J, Zhang T, Prives C. 2001. A subset of tumor-derived mutant forms of p53 down-regulate p63 and p73 through a direct interaction with the p53 core domain. *Mol Cell Biol* **21**: 1874–1887.
- Gu L, Zhu N, Findley HW, Woods WG, Zhou M. 2004. Identification and characterization of the IKK α promoter: Positive and negative regulation by ETS-1 and p53, respectively. *J Biol Chem* **279**: 52141–52149.
- Gupta S, Stamatoyannopoulos JA, Bailey TL, Noble WS. 2007. Quantifying similarity between motifs. *Genome Biol* **8**: R24. doi: 10.1186/gb-2007-8-2-r24.
- Hoh J, Jin S, Parrado T, Edington J, Levine AJ, Ott J. 2002. The p53MH algorithm and its application in detecting p53-responsive genes. *Proc Natl Acad Sci* **99**: 8467–8472.
- Hollenhorst PC, Chandler KJ, Poulsen RL, Johnson WE, Speck NA, Graves BJ. 2009. DNA specificity determinants associate with distinct transcription factor functions. *PLoS Genet* **5**: e1000778. doi: 10.1371/journal.pgen.1000778.
- Hollenhorst PC, McIntosh LP, Graves BJ. 2011. Genomic and biochemical insights into the specificity of ETS transcription factors. *Annu Rev Biochem* **80**: 437–471.
- Huang da W, Sherman BT, Lempicki RA. 2009. Systematic and integrative analysis of large gene lists using DAVID bioinformatics resources. *Nat Protoc* **4**: 44–57.
- Irwin MS, Kondo K, Marin MC, Cheng LS, Hahn WC, Kaelin WG Jr. 2003. Chemosensitivity linked to p73 function. *Cancer Cell* **3**: 403–410.
- Kern SE, Kinzler KW, Bruskin A, Jarosz D, Friedman P, Prives C, Vogelstein B. 1991. Identification of p53 as a sequence-specific DNA-binding protein. *Science* **252**: 1708–1711.
- Kim E, Gunther W, Yoshizato K, Meissner H, Zapf S, Nusing RM, Yamamoto H, Van Meir EG, Deppert W, Giese A. 2003. Tumor suppressor p53 inhibits transcriptional activation of invasion gene thromboxane synthase mediated by the proto-oncogenic factor ets-1. *Oncogene* **22**: 7716–7727.
- Lang GA, Iwakuma T, Suh YA, Liu G, Rao VA, Parant JM, Valentin-Vega YA, Terzian T, Caldwell LC, Strong LC, et al. 2004. Gain of function of a p53 hot spot mutation in a mouse model of Li-Fraumeni syndrome. *Cell* **119**: 861–872.
- Li Y, Prives C. 2007. Are interactions with p63 and p73 involved in mutant p53 gain of oncogenic function? *Oncogene* **26**: 2220–2225.
- Li C, Fan S, Owonikoko TK, Khuri FR, Sun SY, Li R. 2011a. Oncogenic role of EAPII in lung cancer development and its activation of the MAPK–ERK pathway. *Oncogene* **30**: 3802–3812.
- Li C, Sun SY, Khuri FR, Li R. 2011b. Pleiotropic functions of EAPII/TTRAP/TDP2: Cancer development, chemoresistance and beyond. *Cell Cycle* **10**: 3274–3283.
- Liu Y, Asch H, Kulesz-Martin MF. 2001. Functional quantification of DNA-binding proteins p53 and estrogen receptor in cells and tumor tissues by DNA affinity immunoblotting. *Cancer Res* **61**: 5402–5406.
- Lozano G, Zambetti GP. 2005. What have animal models taught us about the p53 pathway? *J Pathol* **205**: 206–220.
- Marin MC, Jost CA, Brooks LA, Irwin MS, O'Nions J, Tidy JA, James N, McGregor JM, Harwood CA, Yulug IG, et al. 2000. A common polymorphism acts as an intragenic modifier of mutant p53 behaviour. *Nat Genet* **25**: 47–54.
- Mavrothalassitis G, Ghysdael J. 2000. Proteins of the ETS family with transcriptional repressor activity. *Oncogene* **19**: 6524–6532.
- Muller PA, Caswell PT, Doyle B, Iwanicki MP, Tan EH, Karim S, Lukashchuk N, Gillespie DA, Ludwig RL, Gosselin P, et al. 2009. Mutant p53 drives invasion by promoting integrin recycling. *Cell* **139**: 1327–1341.
- Muller PA, Vousden KH, Norman JC. 2011. p53 and its mutants in tumor cell migration and invasion. *J Cell Biol* **192**: 209–218.
- Pastorcic M, Das HK. 2000. Regulation of transcription of the human presenilin-1 gene by ets transcription factors and the p53 protooncogene. *J Biol Chem* **275**: 34938–34945.
- Pei H, Yordy JS, Leng Q, Zhao Q, Watson DK, Li R. 2003. EAPII interacts with ETS1 and modulates its transcriptional function. *Oncogene* **22**: 2699–2709.
- Pype S, Declercq W, Ibrahimi A, Michiels C, Van Rietschoten JG, Dewulf N, de Boer M, Vandenabeele P, Huylebroeck D, Remacle JE. 2000. TTRAP, a novel protein that associates with CD40, tumor necrosis factor (TNF) receptor-75 and TNF receptor-associated factors (TRAFs), and that inhibits nuclear factor- κ B activation. *J Biol Chem* **275**: 18586–18593.
- Sampath J, Sun D, Kidd VJ, Grenet J, Gandhi A, Shapiro LH, Wang Q, Zambetti GP, Schuetz JD. 2001. Mutant p53 co-operates with ETS and selectively up-regulates human MDR1 not MRP1. *J Biol Chem* **276**: 39359–39367.
- Sankala H, Vaughan C, Wang J, Deb S, Graves PR. 2011. Upregulation of the mitochondrial transport protein, Tim50, by mutant p53 contributes to cell growth and chemoresistance. *Arch Biochem Biophys* **512**: 52–60.
- Smeenk L, van Heeringen SJ, Koeppel M, van Driel MA, Bartels SJ, Akkers RC, Denissov S, Stunnenberg HG, Lohrum M. 2008. Characterization of genome-wide p53-binding sites upon stress response. *Nucleic Acids Res* **36**: 3639–3654.
- Stambolsky P, Tabach Y, Fontemaggi G, Weisz L, Maor-Aloni R, Siegfried Z, Shiff I, Kogan I, Shay M, Kalo E, et al. 2010. Modulation of the vitamin D3 response by cancer-associated mutant p53. *Cancer Cell* **17**: 273–285.
- Strano S, Munarriz E, Rossi M, Cristofanelli B, Shaul Y, Castagnoli L, Levine AJ, Sacchi A, Cesareni G, Oren M, et al. 2000. Physical and functional interaction between p53 mutants and different isoforms of p73. *J Biol Chem* **275**: 29503–29512.
- Strano S, Fontemaggi G, Costanzo A, Rizzo MG, Monti O, Baccarini A, Del Sal G, Levrero M, Sacchi A, Oren M, et al. 2002. Physical interaction with human tumor-derived p53 mutants inhibits p63 activities. *J Biol Chem* **277**: 18817–18826.
- Sun H, Yuan Y, Wu Y, Liu H, Liu JS, Xie H. 2010. Tmod: Toolbox of motif discovery. *Bioinformatics* **26**: 405–407.
- Takahashi T, Nau MM, Chiba I, Birrer MJ, Rosenberg RK, Vinocour M, Levitt M, Pass H, Gazdar AF, Minna JD. 1989. p53: A frequent target for genetic abnormalities in lung cancer. *Science* **246**: 491–494.
- Tseng JE, Rodriguez M, Ro J, Liu D, Hong WK, Mao L. 1999. Gender differences in p53 mutational status in small cell lung cancer. *Cancer Res* **59**: 5666–5670.
- Wei CL, Wu Q, Vega VB, Chiu KP, Ng P, Zhang T, Shahab A, Yong HC, Fu Y, Weng Z, et al. 2006. A global map of p53 transcription-factor binding sites in the human genome. *Cell* **124**: 207–219.

- Weinmann AS, Yan PS, Oberley MJ, Huang TH, Farnham PJ. 2002. Isolating human transcription factor targets by coupling chromatin immunoprecipitation and CpG island microarray analysis. *Genes Dev* **16**: 235–244.
- Weisz L, Zalcenstein A, Stambolsky P, Cohen Y, Goldfinger N, Oren M, Rotter V. 2004. Transactivation of the EGR1 gene contributes to mutant p53 gain of function. *Cancer Res* **64**: 8318–8327.
- Weisz L, Oren M, Rotter V. 2007. Transcription regulation by mutant p53. *Oncogene* **26**: 2202–2211.
- Wistuba II, Gazdar AF, Minna JD. 2001. Molecular genetics of small cell lung carcinoma. *Semin Oncol* **28**: 3–13.
- Xu D, Wilson TJ, Chan D, De Luca E, Zhou J, Hertzog PJ, Kola I. 2002. Ets1 is required for p53 transcriptional activity in UV-induced apoptosis in embryonic stem cells. *EMBO J* **21**: 4081–4093.
- Yan W, Chen X. 2009. Identification of GRO1 as a critical determinant for mutant p53 gain of function. *J Biol Chem* **284**: 12178–12187.
- Yan W, Liu G, Scoumanne A, Chen X. 2008. Suppression of inhibitor of differentiation 2, a target of mutant p53, is required for gain-of-function mutations. *Cancer Res* **68**: 6789–6796.
- Yan L, Zhang D, Chen C, Mao Y, Xie Y, Li Y, Huang Y, Han B. 2009. TP53 Arg72Pro polymorphism and lung cancer risk: A meta-analysis. *Int J Cancer* **125**: 2903–2911.
- Zalcenstein A, Weisz L, Stambolsky P, Bar J, Rotter V, Oren M. 2006. Repression of the MSP/MST-1 gene contributes to the antiapoptotic gain of function of mutant p53. *Oncogene* **25**: 359–369.
- Zeng Z, Cortes-Ledesma F, El Khamisy SF, Caldecott KW. 2011. TDP2/TTRAP is the major 5'-tyrosyl DNA phosphodiesterase activity in vertebrate cells and is critical for cellular resistance to topoisomerase II-induced DNA damage. *J Biol Chem* **286**: 403–409.
- Zucchelli S, Vilotti S, Calligaris R, Lavina ZS, Biagioli M, Foti R, De Maso L, Pinto M, Gorza M, Speretta E, et al. 2009. Aggresome-forming TTRAP mediates pro-apoptotic properties of Parkinson's disease-associated DJ-1 missense mutations. *Cell Death Differ* **16**: 428–438.



Mutant p53 cooperates with ETS2 to promote etoposide resistance

Phi M. Do, Lakshman Varanasi, Songqing Fan, et al.

Genes Dev. 2012, **26**:

Access the most recent version at doi:[10.1101/gad.181685.111](https://doi.org/10.1101/gad.181685.111)

Supplemental Material

<http://genesdev.cshlp.org/content/suppl/2012/04/16/26.8.830.DC1>

References

This article cites 61 articles, 23 of which can be accessed free at:
<http://genesdev.cshlp.org/content/26/8/830.full.html#ref-list-1>

License

Email Alerting Service

Receive free email alerts when new articles cite this article - sign up in the box at the top right corner of the article or [click here](#).

Use CRISPRmod for targeted modulation of endogenous gene expression to validate siRNA data

horizon
a PerkinElmer company